ROZPRAWY INŻYNIERSKIE • ENGINEERING TRANSACTIONS • 33, 4, 423—443, 1985
Polska Akademia Nauk • Instytut Podstawowych Problemów Techniki

ON AN ELASTIC-PLASTIC BEAM WITH THE ROTATION CONSTRAINT AT THE SUPPORT

A. GAWĘCKI (POZNAŃ)

The behaviour of the geometrically linear elastic-plastic beam with the rotation constraint at the support is analysed. The problem considered belongs to the mechanics of systems at unilateral constraints. It appears that there exists an optimum value of the support limit rotation which is associated with the maximum elastic strength of the beam. The elastic strength increase requires slackening or prestressing of the structure, what depends on load position on the beam. The analysis of this problem shows the close qualitative relationship between slackening and prestressing of the structure. In the elastic-plastic range the loading and unloading cycle up to the ultimate load is considered. It appears that after unloading of the beam when the limit rotations are less than the optimal ones there are no residual deflections and stresses. For a larger value of limit rotations the residual deflections and stresses occur but the stress state after unloading corresponds to that of the reference beam with the optimal rotation constraint. It seems that the observations described in the paper may be utilized in optimization, identification, shakedown and fatigue strength problems.

1. Introduction

Very few solutions are known to unilateral problems of elastic-plastic structures, particularly in the case of boundary constraints. The majority of works mainly focused on elastic structures only. In the range of small displacements there are numerical results for unilaterally supported elastic plates ([1, 2]). Others papers deal with thick beams on elastic Wieghardt foundation [3] and thin elastic plates on rigid foundation, [4]. Particular attention has been paid to geometrically nonlinear problems of elastic beams and plates. Numerical results in the case when unilateral constraints occur in the structure domain have been presented in [5]. Some results for geometrically linear elastic-plastic beams and frames with rotation constraints at the hinge connections are given in [6] and [7].

The present paper deals with the problem of a simple elastic-plastic beam when the angle of the support hinge rotation is constrained. The beam is subjected to the arbitrarily localized concentrated force. The effects of the load position and limit rotation value at the support will be discussed in detail. Considerations are restricted to the geometrically linear thin beam theory.

We assume that the material of the beam is linear elastic-perfectly plastic with the elastic limit σ_E and Young's modulus E (Fig. 1a). The corresponding relationship between the bending moment M and curvature $\varkappa$ is shown in Fig. 1b where M_E and M_Y denote the maximum elastic bending moment and the fully plastic bending moment, respectively. The bending moment — curvature diagram in the case of an ideal I cross-section of the beam — is presented in Fig. 1c.

The beam considered (Fig. 2) is of constant cross-section, namely $EJ = \text{const}$, where J denotes the cross-sectional moment of inertia. The tension fibre due to the positive bending moment action is designated by the dotted line and positively defined rotation corresponds to the deformation caused by the positive bending moment. At the support point *1* (see Fig. 2) the common hinge is applied. At the support point *2* the angle of the rotation is constrained according to the formula

$$M_2 \leqslant 0, \quad \phi_2 - G_2^- \geqslant 0, \quad M_2(\phi_2 - G_2^-) = 0, \tag{1.1}$$

where ϕ_2 denotes the rotation at support *2* and G_2^- is the lower limit rotation at this support. The corresponding mechanical characteristic and the model of this hinge support connection are presented in Fig. 3.

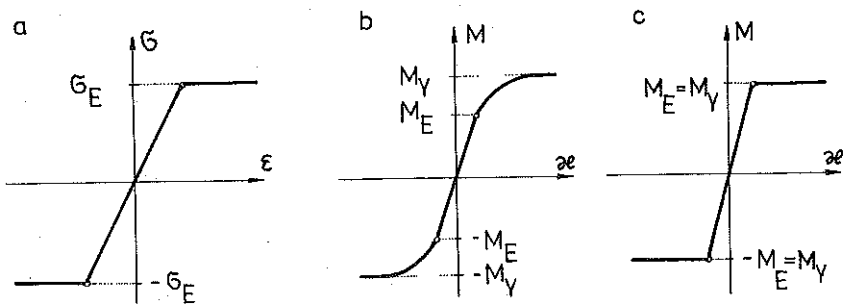

FIG. 1. Mechanical characteristic of the beam: a) $\sigma(\varepsilon)$ diagram for the material of the beam, b) $M(\varkappa)$ diagram for the solid cross-section, c) $M(\varkappa)$ diagram for the ideal I cross-section.

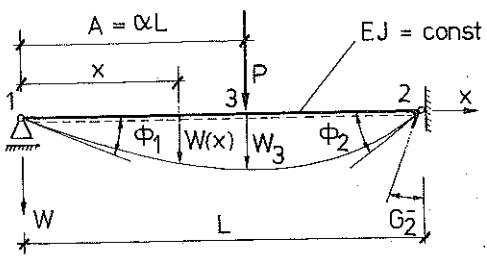

FIG. 2. Beam and load.

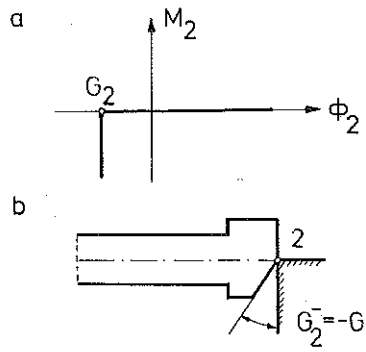

FIG. 3. Unilateral constraint at support 2. a) Mechanical characteristic of support connection, b) Model of support connection.

Beam deformations are caused by an arbitrarily localized concentrated force P and the deflected beam axis is described by the function $W(x)$. Since the beam depth is small, the effects of shear deformations are neglected and, according to Bernoulli's hypothesis, in the coordinate system x, W of Fig. 2 we obtain

$$\phi_2 = W'(L), \qquad \varkappa(x) = -W''(x), \tag{1.2}$$

where primes denote differentiations with respect to x.

The position of the concentrated load P acting at point 3 is determined by the parameter $\alpha = A/L$ where A denotes the load distance from the left hand support 1 and L is the span of the beam. Further considerations are restricted to the cases when load P acts downward.

It is clearly seen that for the small value of P the beam is the pin-pin ended one. For a sufficiently large value of P when the rotation at the support 2 reaches the value of $G_2^- = -G$, the beam becomes the pin-fixed

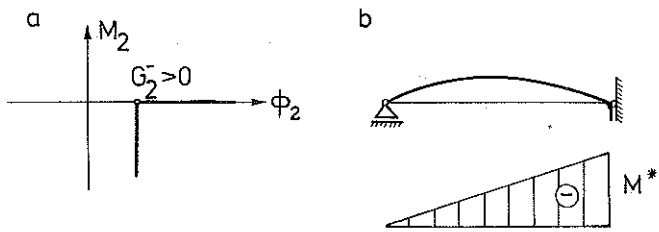

FIG. 4. Prestressing of the beam in the case of $G^- > 0$. a) Mechanical characteristic of the support connection b) Initial strain and stress states.

one. It is worth to notice that for a positive value of G_2^-, even for an unloaded beam, the pin-fixed beam appears and the presence of prestressing is observed. Such a case is shown in Fig. 4.

2. Elastic strength of the beam

The elastic response of the beam corresponds to the cases when the effective stresses are no larger than σ_E. If the shear force influences are neglected, the absolute value of the bending moments at critical points *2* and *3* should be no larger than the maximum elastic one, M_E, namely

$$|M_i| \leqslant M_E, \quad M_E > 0, \quad i = 2, 3$$

or more accurately

$$-M_2 \leqslant M_E, \quad |M_3| \leqslant M_E, \tag{2.1}$$

which follows from the unilateral conditions at support *2*.

For convenience we introduce the following dimensionless notation:

$$\begin{gathered} \xi = x/L, \quad m_i = M_i/M_E, \quad p = PL/M_E, \quad \varphi_i = \phi_i\, EJ/(M_E L), \\ g_i^- = G_i^-\, EJ/(M_E L), \quad w_i = W_i\, EJ/(M_E L^2), \end{gathered} \tag{2.2}$$

where the subscript i denotes the number of the reference critical point. The total values of the bending moment m_i, rotation φ_i and deflection w_i can be expressed by

$$\begin{aligned} m_i &= \sum_{s=0}^{1} m_i^{(s)} = m_i^{(0)} + m_i^{(1)}, \\ \varphi_i &= \sum_{s=0}^{1} \varphi_i^{(s)} = \varphi_i^{(0)} + \varphi_i^{(1)}, \\ w_i &= \sum_{s=0}^{1} w_i^{(s)} = w_i^{(0)} + w_i^{(1)}. \end{aligned} \tag{2.3}$$

In Eq. (2.3) s is the number of the type of the beam. For the pin-pin ended beam $s = 0$ and for the pin-fixed ended beam $s = 1$. In the elastic range the following relations hold:

$$\begin{gathered} s = 0: \quad m_2^{(0)} = 0, \quad m_3^{(0)} = \alpha\,(1-\alpha)\,p, \\ \varphi_1^{(0)} = -\alpha\,(1-\alpha)\,(2-\alpha)\,p/6, \quad \varphi_2^{(0)} = -\alpha\,(1-\alpha^2)\,p/6, \\ w_3^{(0)} = \alpha^2\,(1-\alpha^2)\,p/3; \end{gathered} \tag{2.4}$$

$$s=1: \quad m_2^{(1)} = -\alpha(1-\alpha^2)\,p/2, \quad m_3^{(1)} = \alpha(2+\alpha)(1-\alpha)^2\,p/2,$$

(2.4) [cont.)

$$\varphi_1^{(1)} = -\alpha(1-\alpha)^2\,p/4, \quad \varphi_2^{(1)} = 0,$$

$$w_3^{(1)} = \alpha^2(1-\alpha)^3(3+\alpha)\,p/12.$$

Assuming $g_2 = -g$ and using Eq. (1.1) together with Eqs. (2.4), we can state that the pin-pin ended beam occurs if

$$\varphi_2^{(0)} = -\alpha(1-\alpha^2)\,p/6 > -g,$$

hence

$$\mathrm{p} < p_0(g) = \frac{6g}{\alpha(1-\alpha^2)}. \tag{2.5}$$

For a larger value of p the beam is the pin-fixed one.

In the case of a pin-pin ended beam the bending moment at point *3* reaches its maximum elastic value if the clearance g at support *2* reaches the value of g_0. Thus

$$m_3^{(0)}[p_0(g_0)] = 1.$$

Substituting Eqs. (2.4) and (2.5) into the above relation we obtain

$$g_0 = \frac{1+\alpha}{6} \tag{2.6}$$

and

$$p_0(g_0) = p_{0\max} = \frac{1}{\alpha(1-\alpha)}. \tag{2.7}$$

So for $g \geqslant g_0$ the maximum elastic load p_E is equal to $p_{0\max}$:

$$p_E = p_{0\max} = \frac{1}{\alpha(1-\alpha)}, \quad g \geqslant g_0 = (1+\alpha)/6. \tag{2.8}$$

For $g \leqslant g_0$ the pin-fixed ended beam appears and the minimum or maximum elastic bending moment occurs at point *2* or at point *3*, respectively. In this case the elastic behaviour of the beam is observed if

$$p \leqslant p_E = \min(p_{E_2}, p_{E_3}), \quad g \leqslant g_0 = (1+\alpha)/6, \tag{2.9}$$

where p_{E_2} and p_{E_3} correspond to the conditions $m_2(p_{E_2}) = -1$ and $m_3(p_{E_3}) = 1$, respectively. On the base of Eqs. (2.4) we obtain

$$m_2(p_{E_2}) = -\frac{1}{2}\alpha(1-\alpha^2)[p_{E_2} - p_0(g)] = -1$$

and

$$m_3(p_{E_3}) = m_3^{(0)}[p_0(g)] + m_3^{(1)}[p_{E_3} - p_0(g)] =$$

$$= \alpha(1-\alpha)\, p_0(g) + \frac{1}{2}\alpha(2+\alpha)(1-\alpha)^2 [p_{E_3} - p_0(g)] = 1,$$

hence

$$p_{E_2} = \frac{2(1+3g)}{\alpha(1-\alpha^2)}, \tag{2.10}$$

$$p_{E_3} = \frac{2(1-3\alpha g)}{\alpha(1-\alpha)^2(2+\alpha)}. \tag{2.11}$$

The relations (2.8) and (2.9) together with Eqs. (2.10) and (2.11) describe the boundary of the pure elastic response region of the beam in the p_E, g plane. Geometric interpretation of these equations is shown in Fig. 5. The straight

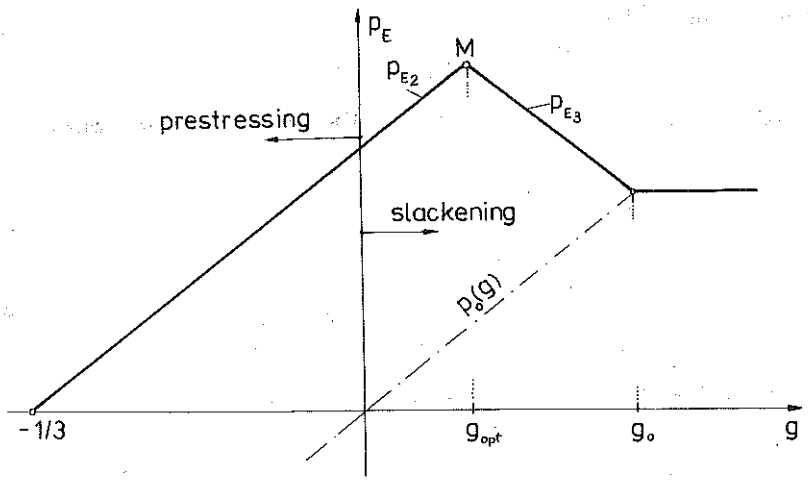

FIG. 5. Elastic load p_E versus limit rotation g at support 2 (case of $\alpha > \alpha_c$).

lines $p_{E_2}(g)$ and $p_{E_3}(g)$ intersect at the point M where the elastic strenght reaches its maximum value $p_{E\max}$. This maximal elastic strength corresponds to the optimum value of limit rotation g_{opt}. The localization of point M is determined by

$$g = g_{\text{opt}}(\alpha) = \frac{(1+\alpha)^2}{6} - \frac{1}{3}, \tag{2.12}$$

$$p_E = p_{E\max}(\alpha) = \frac{1+\alpha}{\alpha(1-\alpha)}. \tag{2.13}$$

This interesting feature of the beam with the support rotation clearance confirms the well-known feeling that a sufficiently small gap is favourable but it is not profitable to have it larger than a certain critical value. The optimal value of g depends on the parameter α which determines the load localization on the beam. Note that for $\alpha < \alpha_c$ the optimal value of the support clearance is negative. In these cases a prestressing of the beam is required and the initial bending moment at support 2 is given by $m_2^* = 3g_{\text{opt}}$. The value of α_c follows from the condition $g_{\text{opt}}(\alpha_c) = 0$, namely

$$\alpha_c = \sqrt{2} - 1 \approx 0.4142. \tag{2.14}$$

The $p_E(g)$ diagram in the case of $\alpha < \alpha_c$ is presented in Fig. 6.

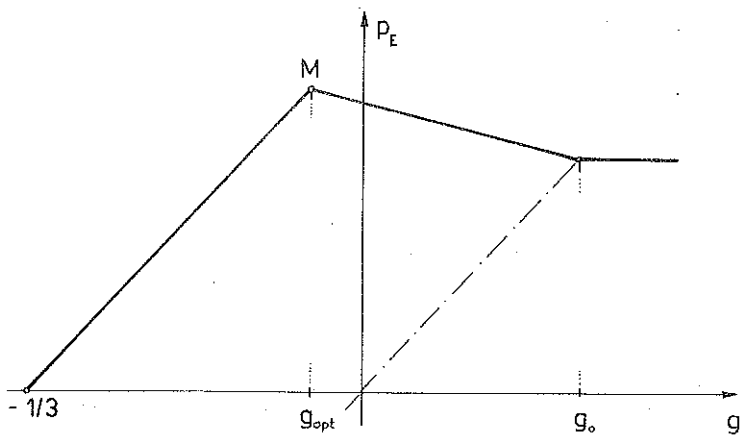

FIG. 6. The $p_E - g$ diagram in the case of $\alpha < \alpha_c$.

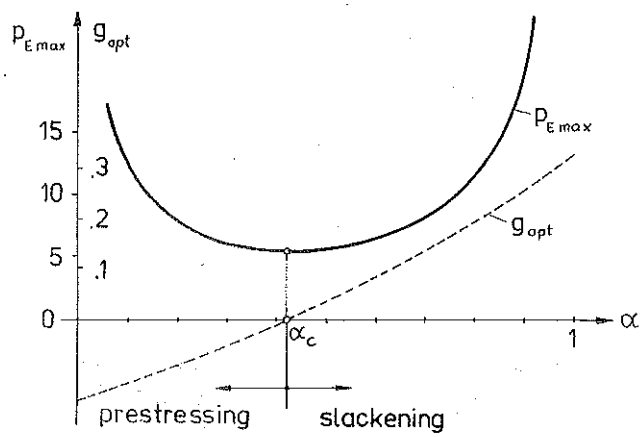

FIG. 7. Maximum elastic load $p_{E\max}(\alpha)$ and optimum value of limit rotation at support 2, $g_{\text{opt}}(\alpha)$.

Now we can conclude that the maximum elastic strength of the beam corresponds to the optimum value of the support limit rotation g_{opt} which depends on the load distribution parameter α. The optimal solution is realized by means of "slackening" or prestressing of the beam. The meaning of the statement expressed above is illustrated in Fig. 7 where $p_{E\max}(\alpha)$ and $g_{opt}(\alpha)$ diagrams are shown. The result obtained here exhibits the significant relationship between prestressing and slackening of the structure at unilateral boundary conditions. The slackening of the structure may be treated as a negative prestressing.

The elastic strength of the optimal solution in comparison to the elastic strength of the pin-fully fixed beam is illustrated by Fig. 8. The corresponding

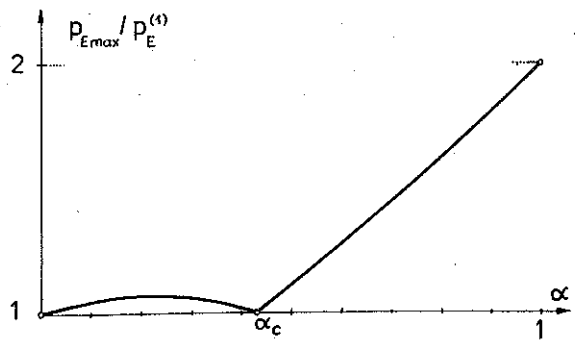

FIG. 8. Maximum elastic load $p_{E\max}$ in comparison to elastic load $p_E^{(1)}$ of pin-fully fixed beam.

formulas are obtained from Eqs. (2.4) and (2.13). Hence

$$p_E^{(1)} = \begin{cases} \dfrac{2}{\alpha(2+\alpha)(1-\alpha)^2}, & \alpha \leqslant \alpha_c, \\ \dfrac{2}{\alpha(1-\alpha^2)}, & \alpha \geqslant \alpha_c, \end{cases} \tag{2.15}$$

thus

$$\frac{p_{E\max}}{p_E^{(1)}} = \begin{cases} \dfrac{(1-\alpha^2)(2+\alpha)}{2}, & \alpha \leqslant \alpha_c, \\ \dfrac{(1+\alpha)^2}{2}, & \alpha \geqslant \alpha_c. \end{cases} \tag{2.16}$$

It is noted that in the case of the standard (bilateral) boundary conditions the prestressing of the pin-fixed beam provides also the increase of the elastic strength. If m_2^* denotes the bending moment at support 2 due to the prestressing, the following relations hold:

$$m_2 = m_2^* - \alpha_2 p, \quad m_3 = \alpha m_2^* + \alpha_3 p,$$

where, according to Eq. (2.4),

$$\alpha_2 = \frac{1}{2}\alpha(1-\alpha^2), \qquad \alpha_3 = \frac{1}{2}\alpha(2+\alpha)(1-\alpha)^2.$$

Consider the problem of maximizing p_E subject to the constraints

a) $m_2^* - \alpha_2 p_E \leqslant 1$,
b) $m_2^* - \alpha_2 p_E \geqslant -1$,
c) $\alpha m_2^* + \alpha_3 p_E \leqslant 1$,
d) $\alpha m_2^* + \alpha_3 p_E \geqslant -1$,
e) $m_2^* \leqslant 1$,
f) $m_2^* \geqslant -1$,
g) $p_E \geqslant 0$.

The admissible region in the p_E, m_2^* plane is presented in Fig. 9. It is clearly seen that the maximum value of p_E corresponds to the point S where

$$p_{E\max} = \frac{1+\alpha}{\alpha(1-\alpha)}, \qquad m_{2\text{opt}}^* = \frac{(1+\alpha)^2}{2} - 1. \tag{2.17}$$

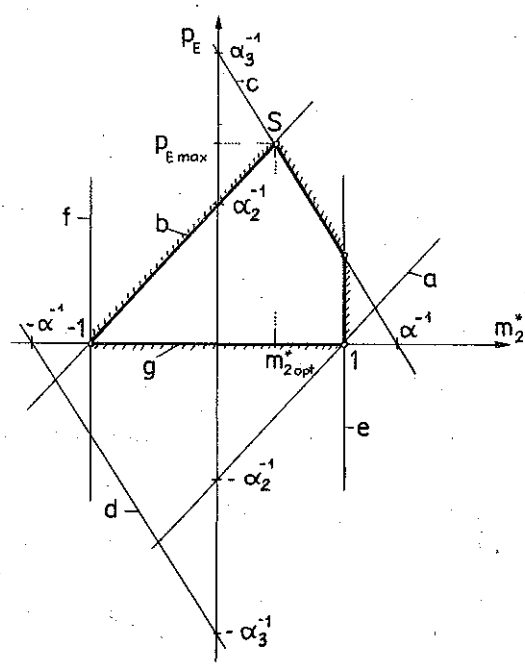

FIG. 9. Graphical solution of maximizing p in the case of prestressing the pin-fully fixed beam.

From Eq. (2.17) it follows that the maximum elastic load in the case of optimal prestressing of the standard pin-fixed beam is identical to that obtained previously for the beam with the optimal rotation constraint at the support 2. Note that $m_2^* \leqslant 0$ if $\alpha \leqslant \alpha_c$ and $m_2^* \geqslant 0$ if $\alpha \geqslant \alpha_c$.

3. Elastic deflections of the beam

The variations of the beam stiffness in the course of elastic deformations appear as essential features of the beam at unilateral constrains. In order to illustrate this problem, consider the relationship between the load p and deflection of the load action point "3". Basing on Eq. (2.4), the following "deflection-load" relation is obtained:

$$\delta(p, g, \alpha) \equiv w_3(p, g, \alpha) = \begin{cases} \frac{1}{3}\alpha^2(1-\alpha)^2 p, & p \leqslant p_0(g, \alpha), \\ \frac{1}{3}\alpha^2(1-\alpha)^2 p_0(g, \alpha) + & \\ \quad + \frac{1}{12}\alpha^2(1-\alpha)^3(3+\alpha)[p - p_0(g, \alpha)], & \\ & p_0(g, \alpha) \leqslant p \leqslant p_E(g, \alpha), \end{cases} \tag{3.1}$$

where, according to the Eqs. (2.5), (2.8), (2.9), (2.10) and (2.11),

$$p_0(g, \alpha) = \frac{6g}{\alpha(1-\alpha^2)}, \tag{3.2}$$

$$p_E(g, \alpha) = \begin{cases} \frac{2(1+3g)}{\alpha(1-\alpha^2)}, & g \leqslant g_{\text{opt}}, \\ \frac{2(1-3\alpha g)}{\alpha(1-\alpha)^2(2+\alpha)}, & g_{\text{opt}} \leqslant g \leqslant g_0, \\ \frac{1}{\alpha(1-\alpha)} = p_0(g_0, \alpha), & g \geqslant g_0 = (1+\alpha)/6. \end{cases} \tag{3.3}$$

Substituting Eq. (3.2) into Eq. (3.1), the deflection–load relation takes the form

$$\delta(p, g, \alpha) = \begin{cases} \frac{1}{3}\alpha^2(1-\alpha)^2 p, & p \leqslant p_0(g, \alpha) \\ \frac{1}{2}\alpha(1-\alpha^2) g + \frac{1}{12}\alpha^2(1-\alpha)^3(3+\alpha) p, & \\ & p_0(g, \alpha) \leqslant p \leqslant p_E(g, \alpha). \end{cases} \tag{3.4}$$

The typical $p-\delta$ diagrams are presented in Fig. 10.

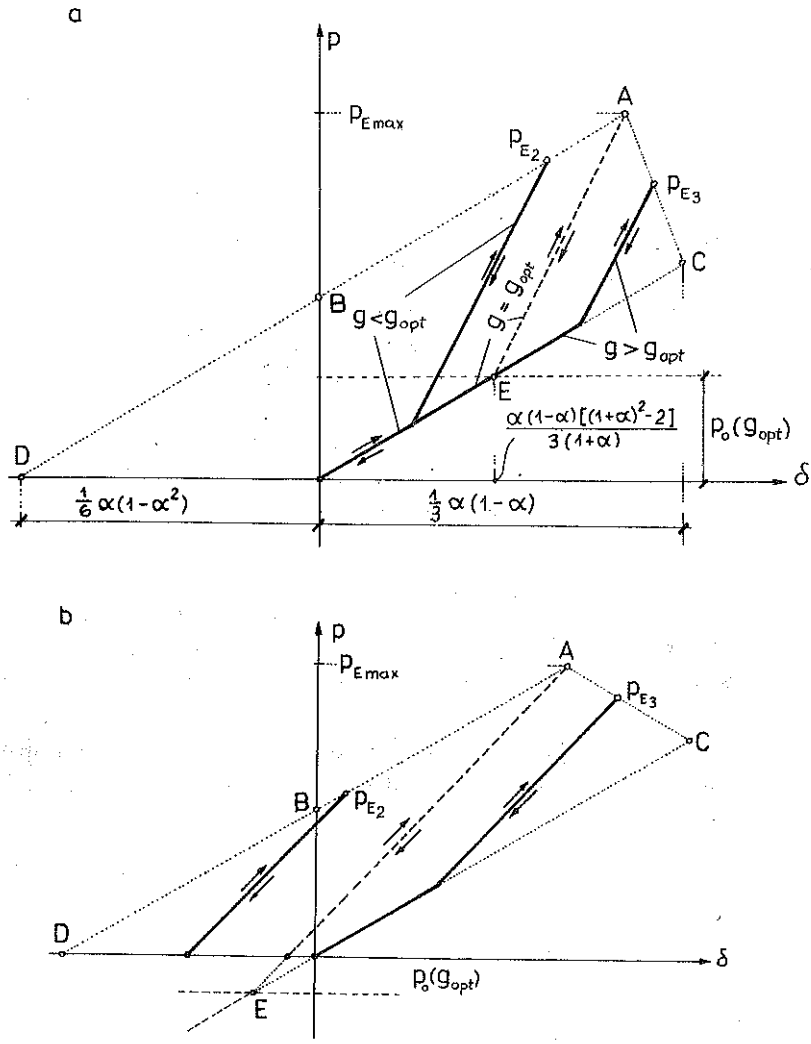

FIG. 10. Load-deflection diagram for the beam with the rotation constraint at support 2: a) case of $\alpha > \alpha_c$, b) case of $\alpha < \alpha_c$.

Taking Eqs. (3.3) and (3.4), one can derive relationships between the elastic load p_E and the corresponding deflection δ_E. For $g \leqslant g_{\text{opt}}$ the following equations are valid:

$$
\begin{aligned}
p_E(g, \alpha) &= \frac{2(1+3g)}{\alpha(1-\alpha^2)}, \\
\delta_E(g, \alpha) &= \frac{\alpha(1-\alpha)}{6(1+\alpha)}[(1-\alpha)(3+\alpha)+12g]
\end{aligned}
\tag{3.5}
$$

and for $g \geqslant g_{\text{opt}}$

$$p_E(g, \alpha) = \frac{2(1-3\alpha g)}{\alpha(1-\alpha)^2(2+\alpha)},$$

(3.6)

$$\delta_E(g, \alpha) = \frac{\alpha(1-\alpha)}{6(2+\alpha)}(3+\alpha+6g).$$

Equations (3.5) and (3.6) represent two straight lines in the p_E, δ_E plane. Eliminating the parameter g we finally obtain

$$g \leqslant g_{\text{opt}}: \quad \delta_E(p_E) = -\frac{1}{6}\alpha(1-\alpha^2)+\frac{1}{3}\alpha^2(1-\alpha)^2 p_E, \tag{3.7}$$

$$g \geqslant g_{\text{opt}}: \quad \delta_E(p_E) = \frac{1}{6}(1-\alpha^2)-\frac{1}{6}\alpha(1-\alpha)^3 p_E. \tag{3.8}$$

Equation (3.7) describes the line ABD and Eq. (3.6) describes the line AC. Using these equations the coordinates of points A, B, C, D may be easily obtained.

In the case of prestressing of the standard pin-fixed beam the deflections depend on the prescribed boundary conditions at support 2. If the optimal prestressing is realized by the suitable rotation of the fixed end of the beam, the $p-\delta$ line for sufficiently large load is identical to that obtained for the beam with the optimal constrained rotation at support 2. This situation is explained in Fig. 11. The initial deflection of the prestressed beam δ^*

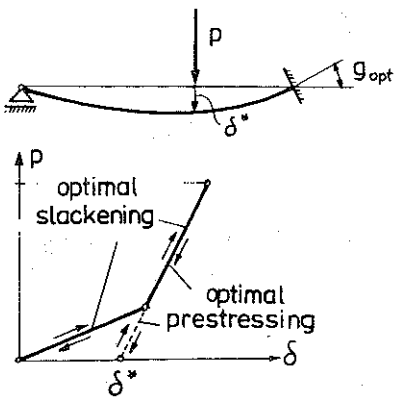

FIG. 11. Initial deflections and $p(\delta)$ diagram for the prestressed beam.

corresponds to the first term in Eq. $(3.4)_2$, namely

$$\delta^* = \frac{1}{2}\alpha(1-\alpha^2) g_{\text{opt}} = \frac{1}{12}\alpha(1-\alpha^2)[(1+\alpha)^2-2]. \tag{3.9}$$

4. Elastic-plastic behaviour of the beam

In the beginning let us concentrate on a limit load problem for the rigid-plastic uniform beam with the rotation constraint at support *2*.

In the presence of the support rotation clearance (i.e. $G > 0$) the way of reaching the ultimate load is not unique. In the range of moderate deflections the yield load $p_L^{(0)}$ occurs and the plastic flow mechanism 0 of the pin-pin ended beam develops (see Fig. 12a). This mechanism is stopped

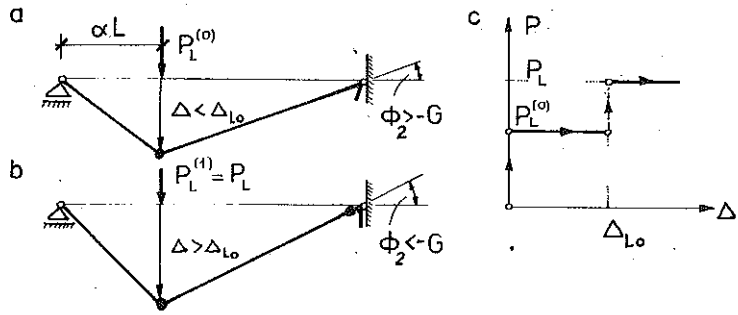

FIG. 12. Rigid-plastic uniform beam with the rotation constraint at support *2*. a) plastic flow mechanism 0, b) plastic flow mechanism *1*, c) load-deflection diagram.

when the hinge rotation at support *2* reaches the value of $-G$ and the deflection of point *3* is equal to $\Delta_{L_0} = (1-\alpha)\,LG$. Then we observe an increase in load up to the value of $P_L^{(1)} = P_L$ which corresponds to the ultimate load of the beam. Further plastic deformations develop according to the plastic flow mechanism *1* typical for the beam built-in at support *2* (Fig. 12b). The corresponding load-deflection diagram where geometry changes are neglected is shown in Fig. 12c. Dimensionless yield loads are given by

$$p_L^{(0)} = \frac{M_Y}{M_E}\,\frac{1}{\alpha\,(1-\alpha)}, \qquad \delta < \delta_{L_0},$$

(4.1)

$$p_L = \frac{M_Y}{M_E}\,\frac{1+\alpha}{\alpha\,(1-\alpha)}, \qquad \delta > \delta_{L_0}$$

where

$$\delta_{L_0} = (1-\alpha)\,g.$$

In the relations (4.1) M_Y denotes the fully plastic bending moment of the beam cross-section and δ is the dimensionless deflection. Note that in the case of g_{opt} for the shape factor $M_Y/M_E = 1$ the ultimate load $p_L(\alpha)$ is equal to the maximum elastic load $p_{E\max}(\alpha)$.

In the case of a negative value of the limit rotation G, the initial position of the beam corresponds to the cantilever beam built-in at support

"2" and the dimensionless deflection of the point "3" is equal to $\delta^* = -(1-\alpha)g$ (Fig. 13a). When the load reaches the value of $p_L(i) = M_Y/[M_E(1-\alpha)]$, then the plastic flow mechanism i occurs. The corresponding bending moment diagram is shown in Fig. 13b. Further deformation develops according to the plastic flow mechanism 1 associated with the ultimate load $p_L^{(1)} = p_L$. Figures 13c, d, and e illustrate the plastic flow mechanism *1*, the bending moment and "load-deflection" diagrams.

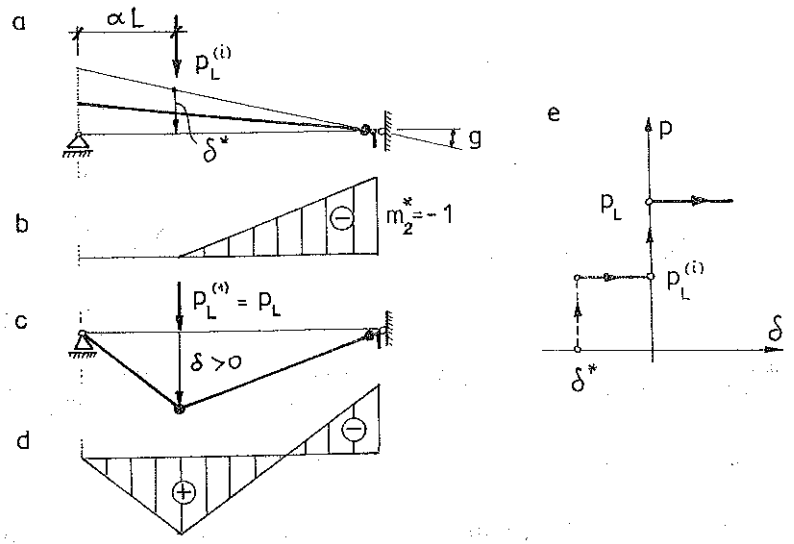

FIG. 13. Rigid-plastic beam with negative rotation constraint at support *2*, a) Initial plastic flow mechanism *i*, b) Initial bending moment diagram, c) Plastic flow mechanism *1*, d) Bending moment diagram, e) $p(\delta)$ diagram.

Passing on to elastic-plastic analysis, for ease of exposition we assume an ideal I cross-section of the beam. In this case $M_Y = M_E$ and for $g = g_{opt}$ the ultimate load p_L is reached in the pure elastic way. For $g \neq g_{opt}$, when the plastic strains arise, there are two deformation modes. The first mode appears for $g < g_{opt}$ when $m_2 = -1$ and $m_3 < 1$. Then the structure stiffness corresponds to the pin-pin ended beam (see Fig. 14a) and the following "deflection-load" relation is valid

$$\delta(p, g, \alpha) = \delta_E(g, \alpha) + \frac{1}{3}\alpha^2(1-\alpha)^2[p - p_E(g, \alpha)], \qquad p_E \leqslant p \leqslant p_L, \tag{4.2}$$

where $\delta_E(g, \alpha)$ and $p_E(g, \alpha)$ are expressed by Eq. (3.7).

The second mode occurs when $g > g_{opt}$ and $m_2 > -1$, $m_3 = 1$. The structure stiffness results from Fig. 14b and the "deflection-load" relation is

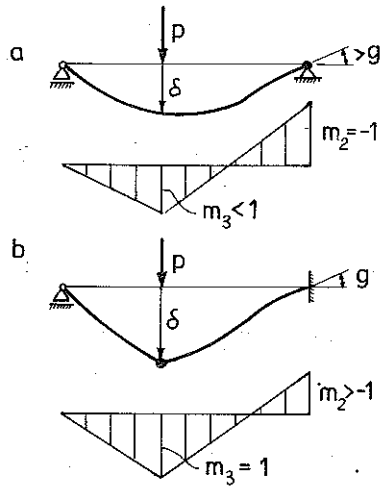

FIG. 14. Beam deformation modes in the elastic-plastic range a) case of $g > g_{\text{opt}}$, b) case of $g < g_{\text{opt}}$.

$$\delta(p, g, \alpha) = \delta_E(g, \alpha) + \frac{1}{3}(1-\alpha)^3 [p - p_E(g, \alpha)], \qquad p_E \leqslant p \leqslant p_L, \tag{4.3}$$

where $\delta_E(g, \alpha)$ and $p_E(g, \alpha)$ are given by Eq. (3.8).

Using Eqs. (4.2) and (4.3) one can compute the deflections δ_L associated with reaching the ultimate load p_L in both cases described above. The final results are

$$\delta_L = \begin{cases} \dfrac{1}{6}\alpha(1-\alpha^2) = \delta_L^-(\alpha), & g \leqslant g_{\text{opt}}, \\ \dfrac{1}{6}(1-\alpha)^2 + (1-\alpha)g = \delta_L^+(g, \alpha), & g \geqslant g_{\text{opt}}. \end{cases} \tag{4.4}$$

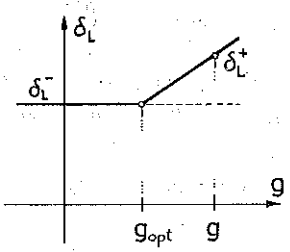

FIG. 15. Yield deflection δ_L versus limit rotation at support 2.

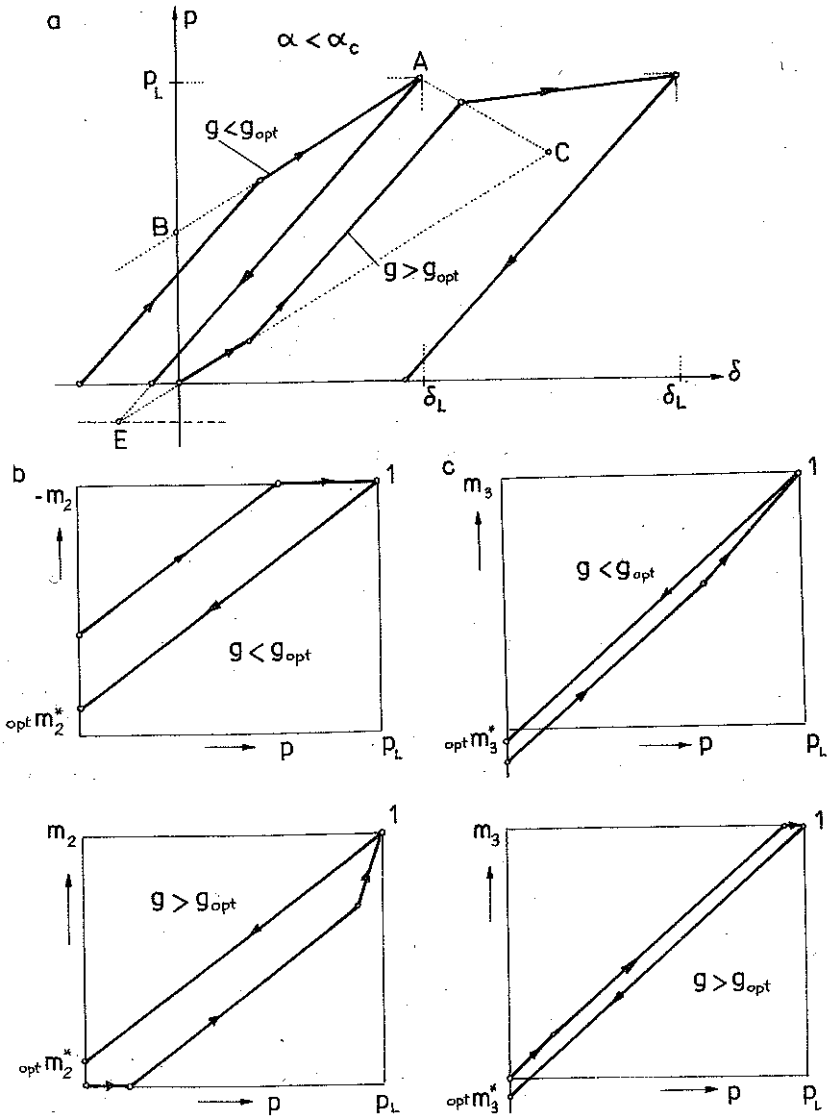

FIG. 16. Loading and unloading cycle (case of $\alpha < \alpha_c$) a) $p(\delta)$ diagrams, b) $m_2(p)$ and $m_3(p)$ diagrams in the case of $g < g_{opt}$, c) $m_2(p)$ and $m_3(p)$ diagrams in the case of $g > g_{opt}$.

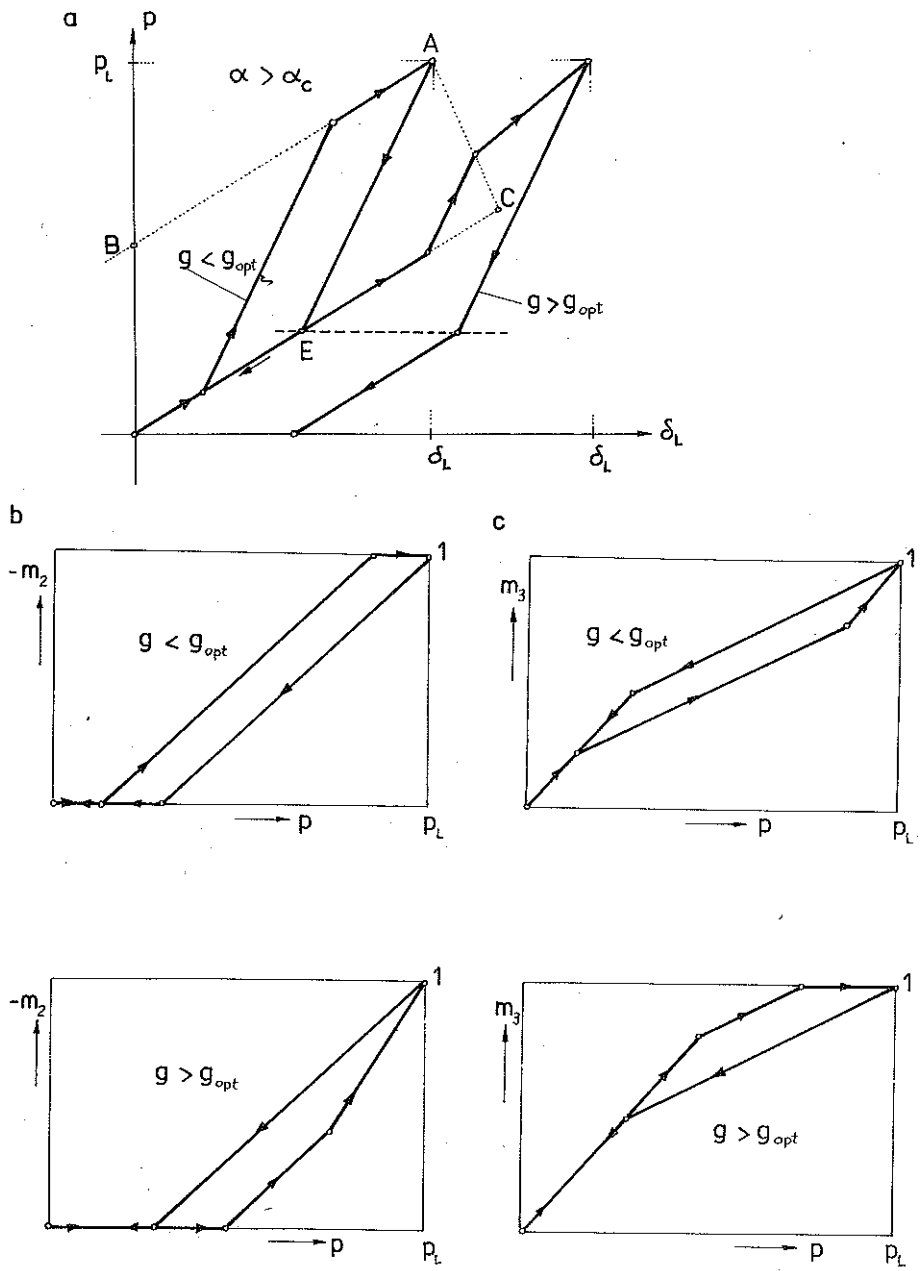

FIG. 17. Loading and unloading cycle (case of $\alpha > \alpha_c$) a) $p(\delta)$ diagrams, b) $m_2(p)$ and $m_3(p)$ diagrams in the case of $g < g_{opt}$, c) $m_2(p)$ and $m_3(p)$ diagrams in the case of $g > g_{opt}$.

Basing on Eq. (4.4), we can state that $\delta_L^- = \delta_L^+$ if $g = g_{opt}$ and $\delta_L^- < \delta_L^+$ if $g > g_{opt}$. So the deflections at the yield point are not less than δ_L^-, namely $\delta_L \geq \delta_L^-$. Note that all cases of $g \leq g_{opt}$ correspond to the same value of $\delta_L = \delta_L^-$. The $\delta_L(g)$ diagram for a given value of α is presented in Fig. 15.

For the sake of illustration, consider the behaviour of the beam throughout the cycle of loading and unloading. In the loading process deflections increase up to δ_L and then the unloading process begins. The cycle is stopped when the load $p = 0$. The final results are gathered in Figs. 16 and 17 where $p(\delta)$, $m_2(p)$ and $m_3(p)$ diagrams are given. Figure 16 is related to the case of $\alpha < \alpha_c$ when the optimal solution corresponds to the prestressing of the beam. The case of $\alpha > \alpha_c$ is illustrated in Fig. 17.

It is clearly seen that the behaviour of the beam throughout the cycle of loading and unloading strongly depends on the limit rotation g. We observe substantial qualitative differences between cases discussed before. In the case of $g < g_{opt}$ the total energy dissipation is concentrated at the right support *2* up to reaching the ultimate load p_L. Therefore there is no residual deflection after unloading. For $g = g_{opt}$ we obtain the particular case in which there are no energy dissipation, residual stresses and deflection. The way of reaching the ultimate load is pure nonlinear elastic. For $g > g_{opt}$, reaching the ultimate load is associated with the energy dissipation at point *3* localized between the supports of the beam. For this reason the residual deflection δ_r remains.

Finally we compare the results obtained here with the solution for the standard pin-fixed ended beam (i.e. bilaterally constrained against rotation at support *2*). The corresponding $p(\delta)$ diagrams for $\alpha > \alpha_c$ are shown in Fig. 18. It is seen that the elastic strength increase for the beam with optimal clearance at the support is associated with the considerable decrease of the beam stiffness. In other words, the elastic strength increase requires suitable

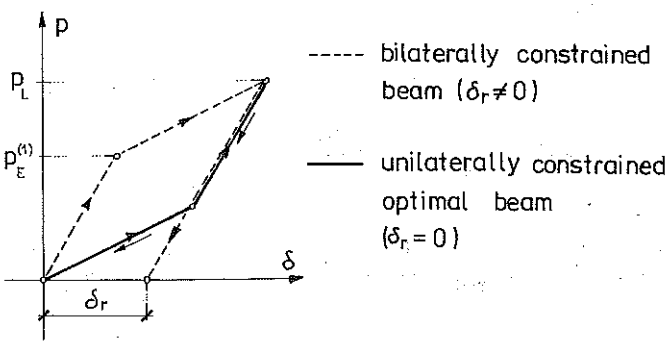

FIG. 18. Load-deflection diagrams for the unilaterally and bilaterally constrained pin-fixed beam.

slackening of the structure. This conclusion is valid when the load position corresponds to $\alpha > \alpha_c$. In the case of $\alpha < \alpha_c$ when the optimal prestressing is applied, the unilaterally constrained beam stiffness is identical to that of the reference optimal prestressed beam at bilateral boundary constraints.

5. Concluding remarks

The problem of an elastic-plastic beam in the presence of clearances at the support is of theoretical and practical importance. The analysis of this simple structure leads to some unexpected results. The considerable strength increase and nonlinear behaviour of the beam appear as essential features in the range of elastic deformations. The examples presented in the work demonstrate the close qualitative relationship between slackening and prestressing of a structure. More detailed analysis shows that there exists an optimum value of the limit support rotation for which the elastic strength reaches its maximum. The elastic strength increase requires, the suitable slackening of a structure. It seems that the observations described above may be utilized in fatigue strength, optimization and identification problems.

The behaviour of the beam at unilateral support constraints in the range of elastic-plastic deformations is not typical. In the course of loading and unloading cycle one can observe the variability of the beam stiffness. For I cross-section of the beam in the case of optimal rotation constraints at the support the way of reaching the ultimate load is pure nonlinear elastic. If the rotation constraint is less than the optimal one, the plastic deformations concentrate at the fixed end and after unloading there are no residual stresses and residual deflections; moreover, the clearance at the support due to plastic deformations becomes the optimal one.

In the case when the support rotation constraint is larger than the optimal one, some unfavourable effects are noted as relatively small stiffness and residual deflections. For arbitrary values of limit rotation, however, the residual stress state after unloading corresponds to the case of a beam with optimal limit rotation. In other words, we observe an adaptation of the beam to the optimal stress conditions.

The work presented may explain some effects occurring in real structures when connection slackenings result from exploitation processes.

References

1. L. M. Kerr, A. F. Mak, *Loss of contact in the vicinity of a right-angle corner for simply supported laterally loaded plate*, J. Appl. Mech., **48**, 597–600, 1981.

2. A. A. CANNAROZZI, A. TRIALLI, *On the analysis of uniterally supported plates by finite element models*, I. J. Solid and Structure, **20**, 2, 179–189, 1984.
3. J. MĄCZKA, *Wyznaczanie obszarów kontaktu belki podpartej oddziaływującej z podłożem typu Wieghardta*, Arch. Inżyn. Ląd., **17**, 2, 391–402, 1971.
4. A. A. CANNAROZZI, *On the resolution of some unilaterally constrained problems in structural engineering*, Comp. Meth. in Appl. Mech. and Engg., **24**, 339–357, 1980.
5. K. OHTAKE, J. T. ODEN, N. KIKUCHI, *Analysis of certain unilateral problem in von Kármán plate theory by a penalty method. Part 2. Approximation and numerical analysis*, Comp. Meth. in Appl. Mech. and Engg., **24**, 317–337, 1980.
6. A. GAWĘCKI, *Nonlinear effects of joint clearances on behaviour of bar structures*, 24th Polish Solid Mechanics Conference, Jachranka, 22–27 August 1983.
7. A. GAWĘCKI, *Elastic-plastic beams and frames with unilateral boundary conditions*, J. Struct. Mech. [in press].

STRESZCZENIE

O BELCE SPRĘŻYSTO-PLASTYCZNEJ Z OGRANICZENIEM OBROTU NA PODPORZE

W pracy przeanalizowano wpływ ograniczenia kąta obrotu przekroju podporowego na zachowanie się belki sprężysto-plastycznej w zakresie małych przemieszczeń. Rozważane zadanie należy do mechaniki układów z więzami jednostronnymi. Okazuje się, że istnieje pewna optymalna wartość luzu podporowego odpowiadająca maksymalnej nośności sprężystej belki. W zależności od umiejscowienia siły skupionej, stanowiącej obciążenie belki, podwyższenie nośności sprężystej wymaga albo rozluźnienia albo wstępnego sprężenia konstrukcji. Analiza tego zagadnienia wykazała ścisłe jakościowe pokrewieństwo zabiegów rozluźniania i sprężania konstrukcji. W obszarze odkształceń sprężysto-plastycznych badano cykl obciążenia i odciążenia dochodząc do nośności granicznej. Okazało się, że po odciążeniu przy luzach mniejszych od wartości optymalnej nie występują ugięcia i naprężenia resztkowe. Dla większych wartości luzów resztkowe ugięcia i naprężenia pojawiają się, jednak stan naprężenia po odciążeniu belki odpowiada belce o optymalnej wartości luzu. Wydaje się, że spostrzeżenia zawarte w niniejszej pracy mogą znaleźć zastosowanie w problemach optymalizacji, identyfikacji, przystosowania konstrukcji oraz wytrzymałości zmęczeniowej.

РЕЗЮМЕ

ОБ УПРУГОПЛАСТИЧЕСКОЙ БАЛКЕ С ОРГАНИЧЕНИЕМ ВРАЩЕНИЯ НА ОПОРЕ

В работе проанализировано влияние ограничения угла вращения сечения опоры на поведение упругопластической балки в области малых перемещений. Рассматриваемая задача принадлежит к механике систем с односторонними связями. Оказывается, что существует некоторое оптимальное значение зазора опоры, отвечающее максимальной несущей способности упругой балки. В зависимости от расположения сосредоточенной силы, составляющей нагружение балки, повышение упругой несущей способности требует или ослабления, или предварительного напряжения конструкции. Анализ этой

задачи показал точную качественную аналогию приемов ослабления и напряжения конструкции. В области упругопластических деформаций исследован цикл нагрузки и разгрузки, приходя к предельной несущей способности. Оказывается, что после разгрузки, при зазорах меньших чем оптимальное значение, не выступают остаточные прогибы и напряжения. Для больших значений зазоров остаточные прогибы и напряжения появляются, однако напряженное состояние после разгрузки балки отвечает балке с оптимальным значением зазора. Кажется, что замечания, содержавшиеся в настоящей работе, могут найти применение в проблемах отпимизации, идентификации, приспособления конструкции и усталостной прочности.

TECHNICAL UNIVERSITY OF POZNAŃ

Received April 19, 1985.